

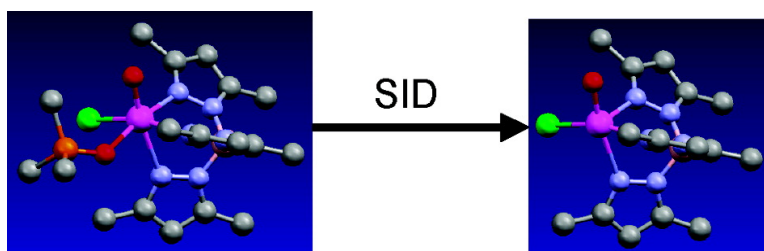
Communication

Isolation, Characterization of an Intermediate in an Oxygen Atom-Transfer Reaction, and the Determination of the Bond Dissociation Energy

Victor N. Nemykin, Julia Laskin, and Partha Basu

J. Am. Chem. Soc., **2004**, 126 (28), 8604-8605 • DOI: 10.1021/ja049121f • Publication Date (Web): 24 June 2004

Downloaded from <http://pubs.acs.org> on March 31, 2009



More About This Article

Additional resources and features associated with this article are available within the HTML version:

- Supporting Information
- Links to the 1 articles that cite this article, as of the time of this article download
- Access to high resolution figures
- Links to articles and content related to this article
- Copyright permission to reproduce figures and/or text from this article

[View the Full Text HTML](#)



ACS Publications
 High quality. High impact.

Isolation, Characterization of an Intermediate in an Oxygen Atom-Transfer Reaction, and the Determination of the Bond Dissociation Energy

Victor N. Nemykin,[†] Julia Laskin,^{*,‡} and Partha Basu^{*,†}

Department of Chemistry and Biochemistry, Duquesne University, Pittsburgh, Pennsylvania 15282, and
Chemical Sciences Division, Pacific Northwest National Laboratory, Richland, Washington 99352

Received February 17, 2004; E-mail: basu@duq.edu; Julia.Laskin@pnl.gov

Redox reactions coupled with the formal loss or gain of an oxygen atom are ubiquitous in chemical processes. Such reactions proceed through the reduction of the donor center (XO) and the oxidation of the acceptor (Y) molecule.^{1–3} Among many examples of the metal-centered oxygen atom transfer (OAT) reactivity, those involving molybdenum complexes have been widely investigated due to their involvement in mononuclear molybdenum enzymes.⁴ The heat of reaction of the overall atom transfer process can be expressed as a difference between the bond dissociation energies (BDEs) of the oxygen-donor (X) and oxygen-acceptor (Y) bond, i.e., $\Delta H = D_{X=O} - D_{Y=O}$.⁵

It has recently become apparent that the OAT reactions from many $[\text{MoO}_2]^{2+}$ cores proceed via multiple steps.⁶ Here we describe the isolation and characterization of an intermediate of OAT reaction, $\text{LMoO}(\text{OPMe}_3)\text{Cl}$ (**1**), (where L = hydrotris(3,5-dimethyl-1-pyrazolyl)borate ligand) generated by reacting LMoO_2Cl with PMe_3 . Surface-induced dissociation (SID) of the complex was studied using a novel Fourier transform ion cyclotron resonance mass spectrometer (FT-ICR MS) specially configured for SID experiments.⁷ The Mo–OPMe₃ BDE was determined using RRRKM modeling of the time- and energy-dependent SID data. The determination of the BDE allows description of the overall heat of the reaction in a stepwise fashion for the first time.

Room-temperature anaerobic reaction of LMoO_2Cl with PMe_3 in benzene resulted in a rapid change in color from light yellow to dark green. The target compound, **1**, has been precipitated as a crystalline solid by adding hexane into the reaction mixture (Supporting Information). The compound is soluble in acetonitrile and benzene but decomposes over a period of time. In the solid state, however, the compound is relatively stable.

X-ray quality single crystals (Supporting Information) were grown by slow diffusion of hexane into a solution of benzene. A thermal ellipsoid diagram of the molecular structure is shown in Figure 1. The Mo–N distances are consistent with other reported structures of oxo–Mo(IV) of hydrotrispyrazolyl borate complexes.^{6,8} Compared to the average of the equatorial Mo–N distances, the Mo–N (trans to the terminal oxo group) has been elongated by 0.23 Å. The Mo=O distance of 1.727 Å is significantly shorter than the Mo–O(P) distance (2.139 Å), indicating a reduction in the bond order consistent with a reduced molybdenum center. The phosphorus-to-oxygen distance of 1.492 Å is also consistent with the formation of a P–O double bond. The O(t)–Mo–O–P torsion angle of 46° is smaller than the angle reported for $\text{L}^i\text{PrMoO}(\text{OPeEt}_3)(\text{OPh})$.⁶

Collision-energy resolved SID spectra for **1** are shown in Figure 2. The ions of **1** were produced in a high-transmission electrospray (ESI) source that allowed external accumulation of mass-selected ions prior to their collision with a surface. The ions were then

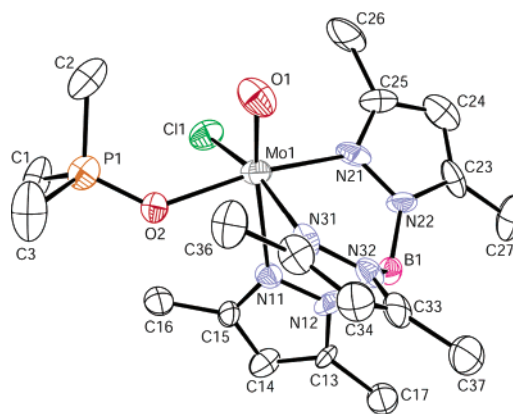


Figure 1. Thermal ellipsoid (30% probability) diagram of **1**. Selected bond distances and angles: Mo(1)–O(1) 1.727(12), Mo(1)–O(2) 2.139(11), Mo(1)–N(11) 2.382(14), Mo(1)–N(31) 2.183(15), Mo(1)–N(21) 2.124(16), Mo(1)–Cl(1) 2.422(6), O(1)–Mo(1)–O(2) 96.3(5), O(1)–Mo(1)–N(11) 170.1(6), O(1)–Mo(1)–N(31) 93.6(6), Mo(1)–O(2)–P(1) 133.6(6).

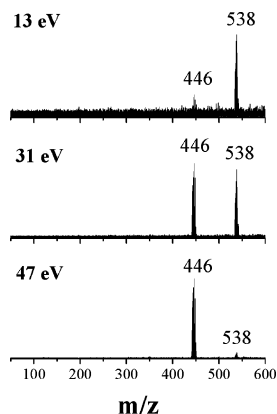


Figure 2. FT-ICR SID spectra of **1** as a function of collision energy for reaction delay of 1 s.

extracted from the source, transferred into the ICR cell using an electrostatic ion guide, and collided with a surface (a self-assembled monolayer of dodecanethiol (HSAM) on Au {111} crystal).⁹ Scattered ions were collected and analyzed in the ICR cell.¹⁰ Relative abundance of the precursor ion and its fragments were recorded at different collision energies and reaction times. The only product ion observed at m/z 446 corresponds to cleavage of the Mo–OPMe₃ bond. Survival curves (SCs) displaying the relative abundance of the precursor ion as a function of collision energy are shown in Figure 3 for four different reaction times (1ms, 10ms, 0.1s, and 1s). The curves corresponding to a longer reaction time are slightly shifted to lower collision energies as a result of the decrease in the kinetic shift. SCs were modeled using a previously described modeling approach¹¹ that utilizes RRRKM theory and a

[†] Duquesne University.

[‡] Pacific Northwest National Laboratory.

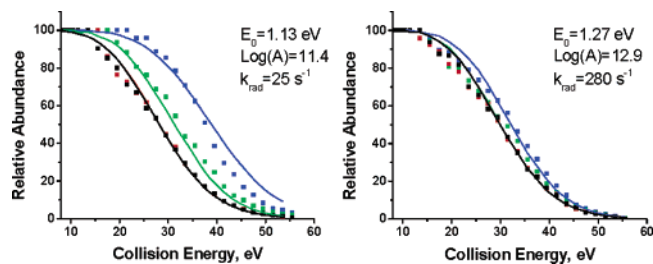


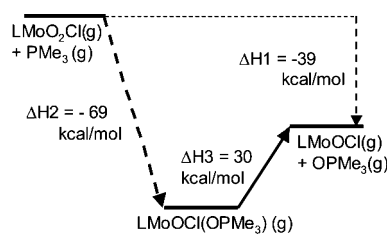
Figure 3. Experimental (points) and simulated (lines) survival curves for protonated leucine enkephalin (left panel) and **1** (right panel) for reaction times of 1 ms (blue), 10 ms (green), 100 ms (red), 1 s (black).

proposed analytical form for the internal energy deposition function (EDF) that represents the internal energy distribution of ions excited by collisions with a surface. Under the same experimental conditions, the EDF for protonated leucine enkephalin, an extensively studied peptide ion of a similar complexity with similar molecular weight (m/z 556) as **1**, was used to establish the energy-transfer efficiency in collision of ions with the HSAM surface. The preexponential factors (A) at 500 K were calculated from the corresponding reaction entropies to provide a link with thermal data. Dissociation parameters obtained from the best fit for leucine enkephalin are in a good agreement with literature data ($E_a = 1.11$ eV, $\log A = 10.7$).¹² SCs for **1** were modeled using the same parameters for the EDF, which correspond to an average kinetic-to-internal energy transfer of 8.9%. This value is in good agreement with the literature data for energy-transfer efficiency for a variety of precursor ions colliding with HSAM surfaces.¹³ Bond dissociation energy of 1.27 eV (29.5 ± 3.5 kcal/mol) was obtained for the Mo–O bond in the intermediate complex. The radiative rate constant for the Mo complex ($k_{\text{rad}} = 280$ s $^{-1}$) is about 10 times higher than the corresponding rate constant for leucine enkephalin ($k_{\text{rad}} = 25$ s $^{-1}$). We used the calculated¹⁴ IR transition intensities for **1** to estimate the radiative rate constant.¹⁵ Good correspondence between the estimated value of 200 s $^{-1}$ and the value obtained from our modeling (280 s $^{-1}$) provides additional support for the accuracy of the model utilized in this study.

The BDE for Mo=O bond was estimated on the basis of the literature data. Watt et al.¹⁶ have determined the BDE for an Mo(VI)=O bond of +96 kcal/mol for $\text{MoO}_2(\text{S}_2\text{CNET}_2)_2$, while Luo et al.¹⁷ determined the BDE of 110 kcal/mol for the Mo(IV)=O bond in an oxometalocene complex. Assuming the BDE for Mo=O bond of 100 kcal/mol and using the literature BDE value for O=PMe₃ bond of 139 kcal/mol,¹⁸ the relative thermodynamic driving force for the formation and the decomposition of the intermediate complex could be calculated. A corresponding thermochemical cycle is shown in Scheme 1 (also in Supporting Information), from which one obtains the heat of reaction for the formation of the intermediate (ΔH_2) –68.5 kcal/mol, and the heat of reaction for the dissociation (ΔH_3) of the Mo–OPMe₃ bond is 29.5 kcal/mol. Thus, the formation of the intermediate is the primary contributing factor to the overall heat of reaction. This methodology presents the first approach toward determining the thermodynamic propensity of the OAT reaction in elementary steps.

In summary, in this study we presented synthesis and characterization of an intermediate complex for an OAT reaction, demonstrating the presence of two steps in the OAT reaction.

Scheme 1



Accurate BDE for the Mo–OPMe₃ bond was determined using FT-ICR SID experiments. The determination of the BDE allows us to establish the thermodynamic propensity for individual steps of the OAT reaction. The results show that in this particular case the heat of formation of the intermediate complex has the major contribution to the overall driving force of the OAT reaction. Future studies in our laboratories will focus on factors that affect the thermochemistry of individual steps in OAT reactions.

Acknowledgment. This work has been partially supported by the National Institutes of Health (P.B.). SID studies were performed at the W.R. Wiley Environmental Molecular Sciences Laboratory, a national scientific user facility sponsored by the U.S. Department of Energy's Office of Biological and Environmental Research and located at Pacific Northwest National Laboratory. PNNL is operated by Battelle for the U.S. Department of Energy. Research at EMSL was carried out within the project 40457 supported by the Office of Basic Energy Sciences of the US Department of Energy.

Supporting Information Available: An X-ray crystallographic file in CIF format and experimental, crystallographic, and computational details. This material is available free of charge via the Internet at <http://pubs.acs.org>.

References

- Holm, R. H. *Chem. Rev.* **1987**, *87*, 1401–1449.
- Woo, L. K. *Chem. Rev.*, **1993**, *93*, 1125–1136.
- Espenson, J. H. *Adv. Inorg. Chem.* **2003**, *54*, 157–202.
- Enemark, J. H.; Cooney, J. J. A.; Wang, J.-J.; Holm, R. H. *Chem. Rev.* **2004**, *104*, 1175–1200.
- Holm, R. H.; Donahue, J. P. *Polyhedron* **1993**, *12*, 571–589.
- Smith, P. D.; Millar, A. J.; Young, C. G.; Ghosh, A.; Basu, P. *J. Am. Chem. Soc.* **2000**, *122*, 9298–9299.
- Laskin, J.; Denisov, E. V.; Shukla, A. K.; Barlow, S. E.; Futrell, J. H. *Anal. Chem.* **2002**, *74*, 3255.
- Young, C. G.; Roberts, S. A.; Ortega, R. B.; Enemark, J. H. *J. Am. Chem. Soc.* **1987**, *109*, 2938–2946.
- Grill, V.; Shen, J.; Evans, C.; Cooks, R. G. *Rev. Sci. Instrum.* **2001**, *72*, 3149–3179.
- Marshall, A. G.; Hendrickson, C. L.; Jackson, G. S. *Mass Spectrometry Reviews* **1998**, *17*, 1–35.
- Laskin, J.; Byrd, M.; Futrell, J. H., *Int. J. Mass Spectrom.* **2000**, *196*, 285–302; Laskin, J., Futrell, J. H. *J. Phys. Chem. A* **2000**, *104*, 5484–5494.
- Jockusch, R. A.; Paech, K.; Williams, E. R. *J. Phys. Chem. A* **2000**, *104*, 3188–3196.
- Vekey, K.; Somogyi, A.; Wysocki, V. H. *J. Mass Spectrom.* **1995**, *30*, 212–217.
- The details are provided in the Supporting Information. For a general description see: Nemykin, V. N.; Basu, P. *Inorg. Chem.* **2003**, *42*, 4046–4056.
- Dunbar, R. C. *Mass Spectrom. Rev.*, **1992**, *11*, 309–339.
- Watt, G. D.; McDonald, J. W.; Newton, W. E. *J. Less-Common Met.* **1977**, *54*, 415–523.
- Luo, L.; Lanza, G.; Fragala, I. L.; Stern, C. L.; Marks, T. J. *J. Am. Chem. Soc.* **1998**, *120*, 3111–3122.
- Hartley, F. R. Ed. *The Chemistry of Organo Phosphorus Compounds*; Wiley & Sons: New York, 1992; Vol 2, p 17.

JA049121F